



Development of a nanoparticle-based gradient method for simple and fast quantification of bacteria-nanoparticle conjugates

Didem Rodoplu  · Ismail Hakki Boyaci · Ugur Tamer · Zekiye Suludere

Received: 1 December 2019 / Accepted: 25 March 2020 / Published online: 21 April 2020
© Springer Nature B.V. 2020

Abstract Nanoparticles are widely used to separate and detect bacteria by immunoassay techniques. However, there is a great need to develop a new low cost, easy-handling, and fast bacteria quantification method in order to give fast response to patients, when there are limited time and instruments. This article describes a new nanoparticle-based quantification method by using only sucrose

gradient centrifugation and an easy optical setup. First of all, spherical-shaped nanoparticles with different chemical components have been synthesized. Buoyancy tendencies of these nanoparticles and effects of different mediums were examined to obtain moving particle band which is necessary for rate-zonal centrifugation. Optimum gradient and process parameters were determined; then, moving bands of nanoparticle and bacteria-conjugated nanoparticle were analyzed by a software. Migration distance of bacteria-captured nanoparticle bands was found inversely proportional to bacterial concentration. Bacteria-nanoparticle conjugates were characterized by transmission electron microscopy images and zeta potential measurements. The developed method enables non-specific detection and quantification of *E. coli* K-12 within the range of 10^5 – 10^8 cfu/ml, by using chitosan-coated CdTe quantum dots. Chitosan-coated CdTe quantum dots were found advantageous for the easy and fast tracking of bacteria-particle conjugate bands in the developed gradient method with respect to their high bacterial capture, sedimentation rate, and light emission properties. According to our findings, the proposed gradient method was found to be an advantageous bacteria quantification method with limited instrument requirement and 50 min of total detection time in solution.

D. Rodoplu · I. H. Boyaci
Department of Nanotechnology and Nanomedicine, Hacettepe University, Beytepe, 06800 Ankara, Turkey

D. Rodoplu
e-mail: didemrodoplu@gmail.com

I. H. Boyaci (✉)
Department of Food Engineering, Faculty of Engineering, Hacettepe University, Beytepe, 06800 Ankara, Turkey
e-mail: ihb@hacettepe.edu.tr

U. Tamer
Department of Analytical Chemistry, Faculty of Pharmacy, Gazi University, 06330 Ankara, Turkey

Z. Suludere
Department of Biology, Faculty of Science, Gazi University, 06500 Ankara, Turkey

Present Address:

D. Rodoplu
National Health Research Institutes (NHRI), Institute of Biomedical Engineering and Nanomedicine, Zhunan, Miaoli County 35053, Taiwan

Keywords Density gradient centrifugation · Moving bands · Optical density · Nanoparticle · Bacteria · Buoyancy

Introduction

According to the extensiveness of bacterial contamination and infections, there is a worldwide growing attention to investigate cost-effective, simple, sensitive, and rapid bacteria detection methods in different research areas such as public health, food protection, and environmental pollution (Ekici and Dumen 2019; Mezger et al. 2015). The conventional microorganism counting techniques, such as culture plating and biochemical tests, require time-consuming and labor-intensive process. The sensitive detection methods such as polymerase chain reaction (PCR), matrix-assisted laser desorption/ionization time of flight (MALDI-TOF) mass spectrometry, and surface-enhanced Raman spectroscopy (SERS) need sophisticated and expensive instruments (Ou et al. 2019). Therefore, development of new, fast, simple, and low-cost bacteria quantification method is highly desirable.

Nanoparticles are important tools to capture and identify bacteria with specific antibody-antigen interactions. They also enable the detection of bacteria with high sensitivity by enhancing the signal of the transducer (Dogan et al. 2016; Guven et al. 2011). Especially gold and gold-coated magnetic nanoparticles were used to enhance the signal and decrease the limit of detection of the spectroscopy techniques such as SERS and surface plasmon resonance measurements (Baniukevic et al. 2013; Guven et al. 2011; Seo et al. 2015). In addition to this, fluorescent nanoparticles and quantum dots are usually utilized for bacteria detections by microscopy and imaging techniques (Wegner and Hildebrandt 2015).

Density gradient centrifugation is a conventional and easy-handling separation technique for sorting particles and molecules based on their size, shape, and density. This technique has crucial importance for purifying substances depending on buoyancy tendencies of biomolecules in novel biotechnology applications (Buckley et al. 2007; Omi et al. 2017; Portoso et al. 2017; Qi et al. 2015; Suresh et al. 2015). Sucrose, which is a biocompatible and nonionic compound, is one of the first and the best density gradient components for purification of cell organelles. During the density gradient sorting of cells or particles, various bands appear in the sucrose gradient with the denser and larger particle bands migrating further (Schachman 1959). Depending on the physical principles, density gradient separation methods can be distinguished into two major categories.

First, for the “isopycnic” separation, the densities of particles must be selected at a range between the lowest and the highest densities of the column’s gradient (Hu and Chen 2015; Jerri et al. 2010; Mace et al. 2012; Prantner et al. 2012). Particles move to the position in the centrifuge tube at which their density is equal to the density of the gradient medium, and they remain there (Lin et al. 2012; Schachman 1959, Sun et al. 2009; Xiong et al. 2011). Thus, isopycnic technique separates particles such as nucleic acids, proteins, and polysaccharides into zones solely based on their buoyant density differences. In addition, the use of multizone gradient increases the density differences between two adjacent gradient layers and improves the separation limits (Akbulut et al. 2012; Écija-Arenas et al. 2016; Mace et al. 2012). The relative centrifugal force (RCF) and the run time should be enough to separate particles in accordance with their isopycnic points. Besides, excessive centrifugation times have no further effect on the position of the bands (Kowalczyk et al. 2011; Mace et al. 2012).

For the second type, which is “rate-zonal” separation, the density of particles and cells must exceed the density of the gradient medium (Hu and Chen 2015; Kowalczyk et al. 2011). During centrifugation, particles undergo Brownian motion under external forces which are centrifugal force, buoyant force, and viscous drag force. Particles migrate into separated bands (zones) through the gradient depending on the effective mass and frictional factor—or sedimentation rate—of NPs (Sharma et al. 2009).

Buoyant density is a measure of floating tendency of a particle in a solution and is measured by using isopycnic centrifugation. It is known that bulk and buoyant densities of nanoparticles (NPs) are not the intrinsic properties. Bulk densities of granular-structured NPs are measured by dividing the total weight of the NPs into the total volume, which includes particle volume, inter-particle void volume, and internal pore volume (Tay et al. 2017). Similarly, in colloidal systems, surface charge distribution that depends on pH and ionic strength of the surrounding medium affects the stability and surface morphology of NPs and leads to the change in the hydrodynamic diameter and buoyant density (Gao et al. 2012; Rodoplu et al. 2015).

In this paper, low-cost and simple gradient method was examined with a new perspective to propose a new nanoparticle-based bacteria quantification method. The physical basis of this new method relies on buoyancy

and optical density of bacteria-captured nanoparticles in the sucrose gradient. In order to obtain fast tracking of “bacteria-captured NP” band in the gradient, overall conditions of sucrose gradient (concentration, volume, solvent) and centrifugation process parameters (rpm, time) were studied. For the preliminary studies, similar sized and spherical-shaped NPs were synthesized. An optical setup and the MATLAB software were used to determine optical density of gradient bands belong to NP and bacteria-captured NPs. Buoyancy and sedimentation rates of gold nanoparticles (AuNPs), gold-coated magnetite NPs ($\text{Fe}_3\text{O}_4@Au$ NPs), and quantum dots (Qdots) were compared in the sucrose gradient. Particles, which have higher sedimentation rates, were utilized in rate-zonal centrifugation, and the process parameters were optimized. Chitosan-coated mercaptopropionic acid capped CdTe ($\text{CdTe}/\text{MPA}@ch$) Qdots which are stable fluorophores and have brighter emission than fluorescent dyes (Dogan et al. 2016; Yang et al. 2015) were found advantageous for the visual tracking of bacteria-particle conjugate bands. Moreover, $\text{CdTe}/\text{MPA}@ch$ Qdots enable fast quantitative measurement of bacteria-particle conjugate bands due to significant sedimentation velocity change with bacterial concentration.

Materials and methods

Chemicals and reagents

Sucrose ($\text{C}_{12}\text{H}_{22}\text{O}_{11}$, MW 342.3 g/mol) and potassium dihydrogen phosphate (KH_2PO_4) were purchased from J.T. Baker Inc. (Phillipsburg, New Jersey). Tryptic Soy Broth (CASO Bouillon), lactose monohydrate (99%, MW: 360.32), sodium dihydrogen phosphate (Na_2HPO_4), and sodium borohydride (NaBH_4) were purchased from Merck KGaA (Darmstadt, Germany). Cadmium chloride (CdCl_2), potassium chloride (KCl), tetrachloroauric acid (HAuCl_4), perchloric acid (HClO_4), trisodium citrate dihydrate, iron (II) sulphate heptahydrate ($\text{FeSO}_4 \cdot 7\text{H}_2\text{O}$), iron (III) chloride (FeCl_3), hydroxylamine hydrochloride ($\text{NH}_2\text{OH} \cdot \text{HCl}$), albumine, and ethylenediaminetetraacetic acid (EDTA) were obtained from Sigma–Aldrich Inc. (Taufkirchen, Germany). N-(3-dimethylaminopropyl)-N-ethylcarbodiimide hypochloride (EDC), 11-mercaptopundecanoic acid (11-MUA), 2-morpholinoethanesulfonic acid monohydrate (MES),

ethanolamine, 2-mercaptoethanol (2-ME), and sodium chloride were purchased from Sigma–Aldrich Inc. (Steinheim, Germany). N-hydroxysuccinimide (NHS) was obtained from Pierce (Rockford, Illinois). Chitosan was purchased from AcrosOrganics (Geel, Belgium).

All reagents used in the experiments were of analytical grade or better. All aqueous solutions were prepared in ultra-pure (18 M Ω cm) water.

Synthesis of nanoparticles

Gold NPs, gold-coated ferrite NPs, and cadmium telluride (CdTe) Qdots were used since they form stable dispersions in solution (Dogan et al. 2016; Fissan et al. 2014; Gao et al. 2012; Tamer et al. 2010). Gold NPs were synthesized according to the literature procedure (Liu and Lu 2006). Briefly, 3 ml of 0.01 M HAuCl_4 solution was added to 100 ml boiling DI water, and the color of the solution turned to yellow. Then, 4 ml of 38.8 mM sodium citrate solution was added drop wise. Boiling process was maintained until a wine-red color was obtained for the solution. Then, the solution was left at the room temperature to cool down.

The magnetic Fe_3O_4 NPs were prepared using coprecipitation method developed by Tamer et al. (Tamer et al. 2010). Briefly, 1.28 M FeCl_3 and 0.64 M $\text{FeSO}_4 \cdot 7\text{H}_2\text{O}$ were dissolved in deionized (DI) water, and 1 M NaOH was added drop wise and it was subjected to vigorous stirring for more than a 40 min period. The precipitated magnetite was collected on a magnet and they were washed three times with DI water. The resulting iron salt was washed with 2 M HClO_4 and left to dry for 3 h at room temperature under an argon atmosphere. Then, the particles were washed 3 times with DI water to remove the acidic medium. A total of 10 mg Fe_3O_4 was dispersed in 5 ml of DI water by ultrasonic water bath. In another baker, 1 g of EDTA was added to 10 ml of 1 M NaOH solution. This solution was mixed at 1:1 (v/v) ratio, and then centrifuged at 8000 rpm for 10 min and re-dispersed in water. After that, 7 ml of 0.1 M CTAB, 3 ml of 0.01 M HAuCl_4 , and 300 μl of 1 M NaOH were added to this solution. After thorough mixing, 150 mg $\text{NH}_2\text{OH} \cdot \text{HCl}$ was added. Following this process, the solution was retained in the ultrasonic water bath for 12 h.

Chitosan-capped mercaptopropionic acid-modified (CdTe/MPA) Qdots were prepared according to the literature procedure with a slight modification (Dogan et al. 2016). While 25 ml of 0.064 mM CdCl_2 have been

stirred continuously in a single-necked flask, 0.10 g trisodium citrate, 100 μ l of 11.5 M mercaptopropionic acid (MPA), and 0.01 mmol Te (IV) were added to the solution. Then, 50 mg NaBH_4 was added on it. The solution was stirred at 96 °C for 1 h. After cooling down to room temperature, Qdots were precipitated by ethanol, centrifuged, and dried. A 75 mg portion of the Qdot powder was re-dissolved in water (pH 11.4), then heated at 96 °C for 2 h and diluted to 25 ml. Chitosan (100 μ l of 1% (w/v)) dissolved in 1% (v/v) acetic acid was added to a 4.9 ml portion of Qdot solution. The pH was adjusted to 5 by adding 300 μ l of 1 M pH 5 acetate buffer. Then, chitosan-coated Qdots (CdTe/MPA@ch) were vortexed for 1 min to homogenize and sonicated for 10 min.

Surface modification of nanoparticles

Here, 50 mM 11-mercaptopundecanoic acid (11-MUA) solution was prepared in absolute ethanol and mixed with NPs for 18 h at room temperature on a shaker at 140 rpm. To remove unbound 11-MUA, particles were washed twice in ethanol.

The carboxylate groups of NPs were activated through EDC/NHS coupling reaction. A total of 3 mg/ml EDC and 2 mg/ml NHS were added on a particle solution which was taken in 50 mM pH 6.5 MES buffer solution. After 25 min of incubation at 140 rpm shaker, particles were washed twice with 10 mM pH 7.4 PBS. During the stirring and washing procedures, attention was paid not to exceed 40 min for the total activation time.

Optimization of sucrose gradient centrifugation parameters

Sucrose stock solution (800 mg/ml) was prepared by dissolving sucrose in 10 mM pH 7.4 PBS solution. By means of diluting the stock solution with PBS, appropriate sucrose solutions within the range of 10–80% (w/v) were prepared. Discontinuous gradient of sucrose was prepared by successive layering of sucrose solutions upon one another as described earlier in the literature (Xiong et al. 2011). Sucrose gradients were prepared inside 15 ml polypropylene centrifuge tubes (LP Italiana S.p.A., Milano, Italy). Total gradient volume was set to 5 ml; optimum gradient was composed by 1 ml each of 40%, 50%, 60%, 70%, and 80% (w/v) sucrose solutions. Before use, gradients were placed in a

refrigerator for 1 h to cool down to 4 °C. Then, sample suspensions were carefully loaded on top layer of the sucrose gradient using micropipette.

Centrifugation was performed by using the refrigerated centrifuge (VMR International Ltd., Leicestershire, UK) at 4 °C, with a swing rotor. Relative centrifugation force (RCF) was altered between 100 and 2000 \times g, and centrifugation period was in the range of 1–120 min. Different solvent mediums were studied to prevent the unwanted sedimentation of NPs on the tube walls and to maintain Gaussian form of moving narrow band during centrifugation. Thus, 10 mM and 20 mM PBS pH 7.4, and 0.8% (w/v) NaCl were used as solvent medium of sucrose and particles. In addition, the gradient parameters such as sucrose concentrations (10–80% (w/v)), sucrose fraction volumes (1–2 ml), total gradient volume (4–10 ml), and sample parameters, such as particles with different surface compositions and loading sample volumes (50–250 μ l), were optimized.

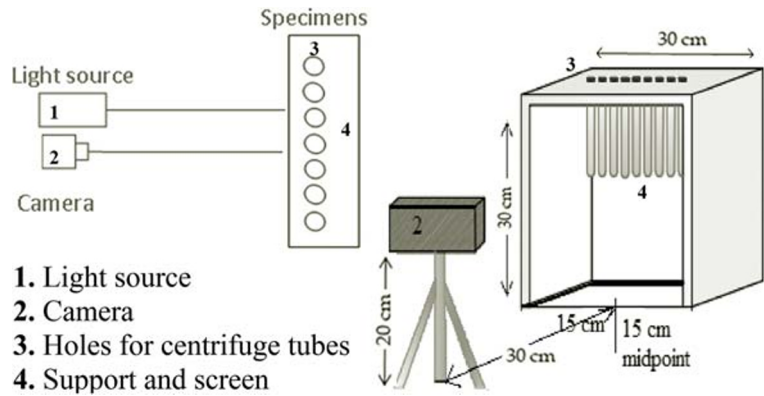
Bacteria immobilization

E. coli K-12 culture which was prepared in Tryptic Soy Broth (CASO Bouillon) medium was incubated at 37 °C for 24 h. Then, *E. coli* K-12 was precipitated at 4500 \times g for 10 min of centrifugation and washed twice with sterilized 10 mM PBS pH 7.4. NPs were incubated with 10^5 – 10^8 cfu/ml of *E. coli* K-12 for 40 min at room temperature on a shaker at 140 rpm. After non-specific bacteria interaction, 200 μ l of each sample were placed on the sucrose gradients without using any washing steps.

Analysis of moving bands

As shown in Fig. 1, gradient tubes were placed in the holes of support after centrifugation. The light source was placed in alignment with the camera, and against the tube supporter and white screen. A commercial 8-megapixel camera was utilized to take digital photographs of the centrifuge tubes. The vertical distance through the gradient was defined from the meniscus of the gradient to the bottom of the centrifuge tube. The optical density values were measured through the vertical distance of each gradient tube. Besides, the migration distances of the moving bands inside the gradient were defined as the distance from the meniscus of the sucrose gradient to the peak of the particle band.

Fig. 1 Schematic representation of optical setup



Photographs of the gradients were taken after every 1–2 min of centrifugation period in order to analyze the slight variations within moving bands and to determine the band migration distances. The photographs belong to Au and magnetite NPs were taken under white light, while CdTe/MPA@ch bands were taken under UV-A dark light ($\lambda = 365$ nm) using a transilluminator (UVP Ltd., Upland, CA).

A picture element (pixel) is represented by three component intensities as red, green, and blue (RGB) (Menesatti et al. 2012). From the photographs, constant interior zones of the tubes were selected as picture element matrixes in order to eliminate the effects of side wall-shape of tubes, and to obtain accurate and repeatable results. These zones were cropped from photographs for the analysis by MATLAB. To draw optical density graphs of AuNP and Fe₃O₄@Au NP, white color was tracked from the pixel matrix. Red color was tracked from the selected matrix to analyze CdTe/MPA@ch Qdot band movements. By using this method, vertical distance-based optical density values for each sample were recorded as optical density graphs.

Characterization of nanoparticles

Transmission electron microscopy (TEM) was used to examine the size and morphology of NP and bacteria-captured NPs. Here, 300 μ l of samples was collected from relevant bands of sucrose gradient. Then, they were rinsed three times with 10 mM pH 7.4 PBS to completely remove sucrose from the solution. TEM samples were prepared by pipette-dripping of 10 μ l of the particle solution onto the TEM grid, allowing it to stand for 10 min and evaporating the solvent in a vacuum. HRTEM instrument (JEOL Ltd., Tokyo, Japan) was run at an accelerating voltage of 120 V.

The zeta potentials of chemically activated NPs and Qdots were measured by ZetaSizer Nanoseries (Malvern Instruments, Worcestershire, UK) at 25 °C. The refractive indexes of gold (0.99), chitosan (1.7), and PBS (1.33) were used for setting the instrument. Samples were diluted to 0.01 mg/mL and 5 experimental runs were performed. All the measurements were performed in triplicates.

Results and discussion

In the present study, a nanoparticle and buoyancy-based bacteria quantification method was presented by means of exploiting the potential of sucrose gradient centrifugation. It is known that size, morphology, and surface compositions of particles have effects on the sedimentation rate and stability of colloidal solutions as a result of Van der Waals forces, electrostatic interactions, and steric forces between binding molecules. The sedimentation rates of NPs in solution and the effects of sucrose gradient parameters (volume, concentration, solvent) on the trends of moving bands were examined in detail by using the developed gradient method.

The buoyancy tendency of “bacteria-captured NPs” increased due to increased bacterial concentration. Therefore, sedimentation rate and the measured migration distance of bacteria-NP bands decreased. Gold-coated-magnetite nanoparticles and quantum dots were chosen to achieve recognizable NP–bacteria band movement in the gradient. Besides, CdTe/MPA@ch Qdots were found advantageous to enumerate bacterial concentration in the range of 10^5 – 10^8 cfu/ml of *E. coli* K-12 by using the gradient of 40%, 50%, 60%, 70%, and 80% (w/v) sucrose dissolved in pH 7.4 PBS medium.

Characterization results of nanoparticles

Buoyancy tendencies of nanoparticles

The buoyancy tendencies of NPs were compared with the optical density–distance graphs of the moving bands after sucrose gradient centrifugation. As can be seen from Fig. 2, AuNP has two moving bands depending on the aggregation of NPs and sucrose concentration of the gradient. Related peaks were identified from the optical density graph (Fig. 2a). The cropped pixel matrix from the photograph of the tube was shown in Fig. 2b. Red and purple colored bands of AuNP were observed at 35% (w/v) sucrose zone and 40–80% (w/v) interface of the gradients, respectively. Even though single NPs and the aggregated ones have the same dry density, due to reduction of surface area/volume ratio and increase on the sedimentation rate in solution, aggregated AuNP purple bands (40–80% w/v sucrose) migrated more than AuNP red bands (35% w/v sucrose). In addition to this, in accordance with the literature, AuNP colors have also turned from red to purple due to particle clustering in ethanol and pH 6.5 MES medium (Liu and Lu 2005; Liu and Lu 2006).

The comparisons of NP band migrations after 45 min of centrifugation at $4149\times g$ in the sucrose gradient were given in Fig. 3. Consequently, both $\text{Fe}_3\text{O}_4@Au$ NPs and CdTe/MPA@ch Qdots were chosen as possible candidates for rate-zonal centrifugation. That is because they moved faster through the 80% w/v sucrose viscosity barrier in 45 min, and they completely precipitated after

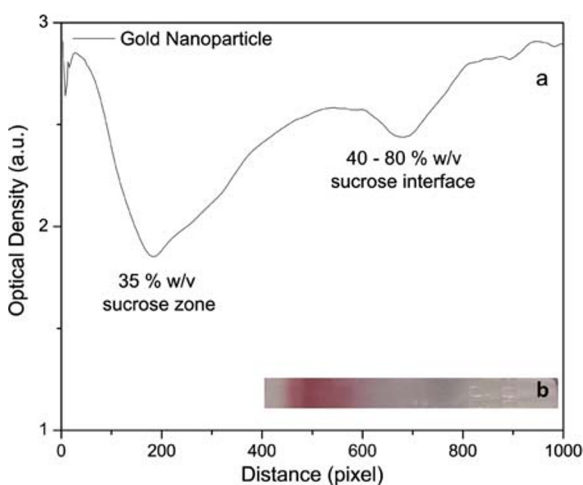


Fig. 2 Optical measurement, **a** optical density graph, and **b** selected pixel matrix of AuNP in the gradient of 30%, 35%, 40%, and 80% (w/v) sucrose, after 45 min of centrifugation at $4149\times g$

120 min of centrifugation. However, Au and Fe_3O_4 NPs remained at the same sucrose zone regardless of centrifugation period. Therefore, buoyant density of AuNP in water medium was predicted to be between 1.12–1.15 g/ml as the density of 30–35% w/v sucrose. Besides, magnetite NPs remained at the 30% w/v sucrose (Fig. 3); thus, buoyant density was predicted as 1.12 g/ml. The buoyant densities were found incomparable with the intrinsic density of elements and bulk density of dry NPs. Densities of gold, iron, and cadmium telluride are known as 19.32 g/ml, 7.87 g/ml, and 5.85 g/ml, respectively (Sik and Grmela 2013; Wolfram Research n.d.) ($d_{Au} > d_{Fe} > d_{CdTe}$). Besides, bulk densities of Au, Fe_3O_4 NPs, and CdTe Qdots are generally known as 1.25 g/ml, 0.84 g/ml, and 6.02 g/ml, respectively (Pathak et al. 2015; US Research Nanomaterials, n.d.-a, b). As a result, it was found that regardless of chemical composition and bulk densities, NPs have showed different band migrations distances with respect to their buoyant densities in different solution.

In order to observe the effects of solvent in detail, AuNPs were taken in water, pH 6.5 50 mM MES, and ethanol, respectively. The migration distances of AuNPs in these solvents were compared in Fig. 3b. As it can be seen, when NPs were taken in pure ethanol and 50 mM pH 6.5 MES buffer, with respect to the increased aggregation, buoyant densities of AuNPs increased above 1.4 g/ml, which is equal to the density of 80% w/v sucrose zone.

Morphological characterization of nanoparticles

The physical morphologies of the NPs were characterized using TEM images (Fig. 4). The spherical-shaped AuNPs' average radii were measured as 13 ± 4 nm (Fig. 4a). TEM images taken before and after sucrose gradient centrifugation of AuNP were given in Fig. 4a and Fig. 4b, respectively. After sucrose gradient centrifugation and washing steps, citrate groups left the medium, and particles showed an aggregation tendency (Fig. 4b).

The average radius of spherical-shaped $\text{Fe}_3\text{O}_4@Au$ NPs was measured as 20 ± 6 nm (Fig. 4c). The average size of the spherical-shaped CdTe/MPA@ch Qdots was measured as 6 ± 1 nm (Fig. 4d). The morphologies and aggregation tendencies of $\text{Fe}_3\text{O}_4@Au$ NPs and CdTe/MPA@ch Qdots remained unchanged after washing steps. In accordance with this, buoyant densities of these NPs remained unchanged. Thus, these particles

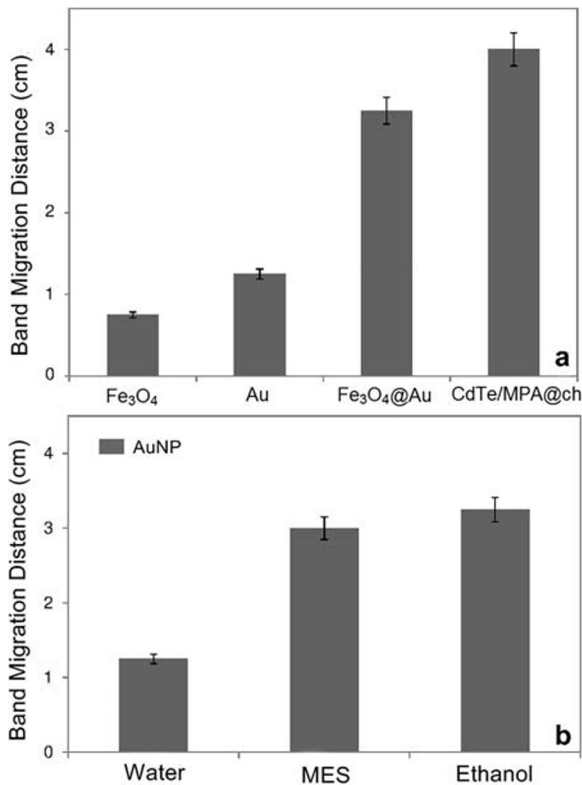


Fig. 3 Band migration distances of different **a** NPs and **b** solvents obtained from the gradient that consist of 30%, 35%, 40%, and 80% (w/v) sucrose, after 45 min of centrifugation at 4149×g

were found appropriate particles for rate-zonal gradient centrifugation.

As can be seen from Fig. 5, morphological structures of *E. coli*-nanoparticle conjugates remained unchanged despite applied centrifugal force and the frictional forces applied by the highly viscous sucrose medium. Bacteria sizes were measured between 2.1 and 2.9 μm (Fig. 5). Because of relatively low centrifugal force and short centrifugation periods were applied, bacteria membrane has not damaged by the internal forces such as tension, shear, and bending forces that affect at the highly viscous 50% (w/v) sucrose medium (Fig. 5a–d) (Amir et al. 2014).

Zeta potential of nanoparticles

The zeta potentials of Fe₃O₄@Au NPs and CdTe/MPA@ch Qdots were measured in pH 7.4 PBS medium (Fig. 6). It is known that particles which have zeta potentials below + 25 mV and above – 25 mV show greater sedimentation tendency with respect to interparticle interactions such as Van der Waals, hydrogen

bonding, and hydrophobic interactions (Kumar and Dixit 2017). Therefore, particles with appropriate surface properties enable moving NP bands without forming pellets in the sucrose gradient medium. From Fig. 6, it was seen that zeta potential of Fe₃O₄@Au NPs (– 9 mV) is higher than that of CdTe/MPA@ch (+ 3 mV) (Fig. 6). Since the zeta potential is between – 5 mV and + 5 mV, CdTe/MPA@ch Qdots which are in flocculation state showed greater sedimentation rate than Fe₃O₄@Au NPs, which are in the early instability state, in the gradient medium.

Besides, it is known that all bacteria with negatively charged cell wall adhere on positively charged surfaces (Li et al. 2019). The non-specific bacterial capture of positively charged CdTe/MPA@ch Qdots is stronger than negatively charged Fe₃O₄@Au NPs, with respect to the ionic bonds formed due to higher electrostatic attraction sites. Therefore, moving bands of bacterial-captured Qdots were predicted to show noticeable variations according to bacterial concentration.

Optimization of gradient parameters

It is necessary to prevent particle sedimentation on the sidewalls of the tube and to obtain moving narrow bands during centrifugation. According to our preliminary results, 200 μl of sample volume and 5 ml of sucrose gradient were found appropriate to obtain moving narrow bands without deformation, such as band extension or dispersion.

In order to observe the effect of gradient medium in detail, 10 mM pH 7.4 PBS, 20 mM pH 7.4 PBS, and 0.8% (w/v) NaCl solutions were utilized to dissolve sucrose, and band migrations in these gradients were compared in Fig. 7. After centrifugation period, narrow bands were disappeared in 20 mM pH 7.4 PBS and 0.8% (w/v) NaCl sucrose solvent mediums, and NPs aggregated and dispersed through the tube side walls. On the other hand, Gaussian forms of NP bands remained unchanged in sucrose gradient that prepared by dissolving in 10 mM PBS medium. Band migration distance showed slight variation during centrifugation period. By virtue of the higher salt concentration, particles moved in the sucrose gradient prepared by 20 mM PBS solution aggregated, and sedimentation was observed on the sidewalls. Even though 0.8% (w/v) NaCl solution has the same NaCl amount with 10 mM PBS solution, due to moving away from

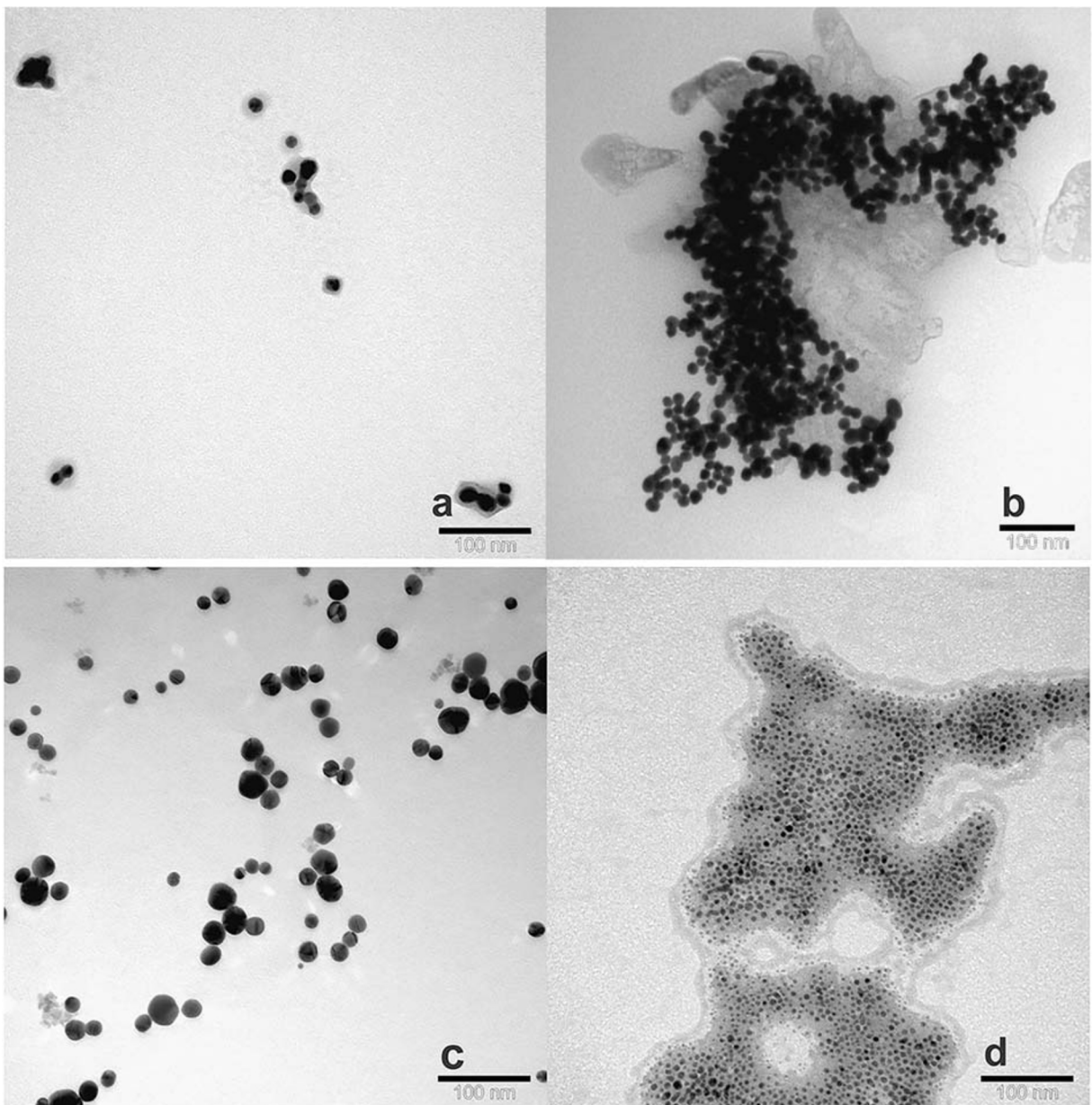


Fig. 4 TEM images of NP bands. **a** AuNP-red band. **b** AuNP-purple band. **c** $\text{Fe}_3\text{O}_4@Au$. **d** CdTe/MPA@ch

isoelectric point of NPs, colloidal stability of the solution decreased. Owing to the increase on the buoyant density and sedimentation rate, NP band prepared in 0.8% (w/v) NaCl migrated more than the NP bands prepared with other solvents. Therefore, 10 mM pH 7.4 PBS was selected as an appropriate solvent to maintain hydrodynamic stability for further bacteria capture studies.

In addition, it was seen that the appropriate gradient parameters to obtain moving bands were changed for each NP that was utilized. For the further bacteria-NP conjugate band migrations with $\text{Fe}_3\text{O}_4@Au$ and CdTe/MPA@ch NPs, more viscous medium that consists of 1 ml each of 40%, 50%, 60%, 70%, and 80% (w/v) sucrose was predicted as an appropriate gradient.

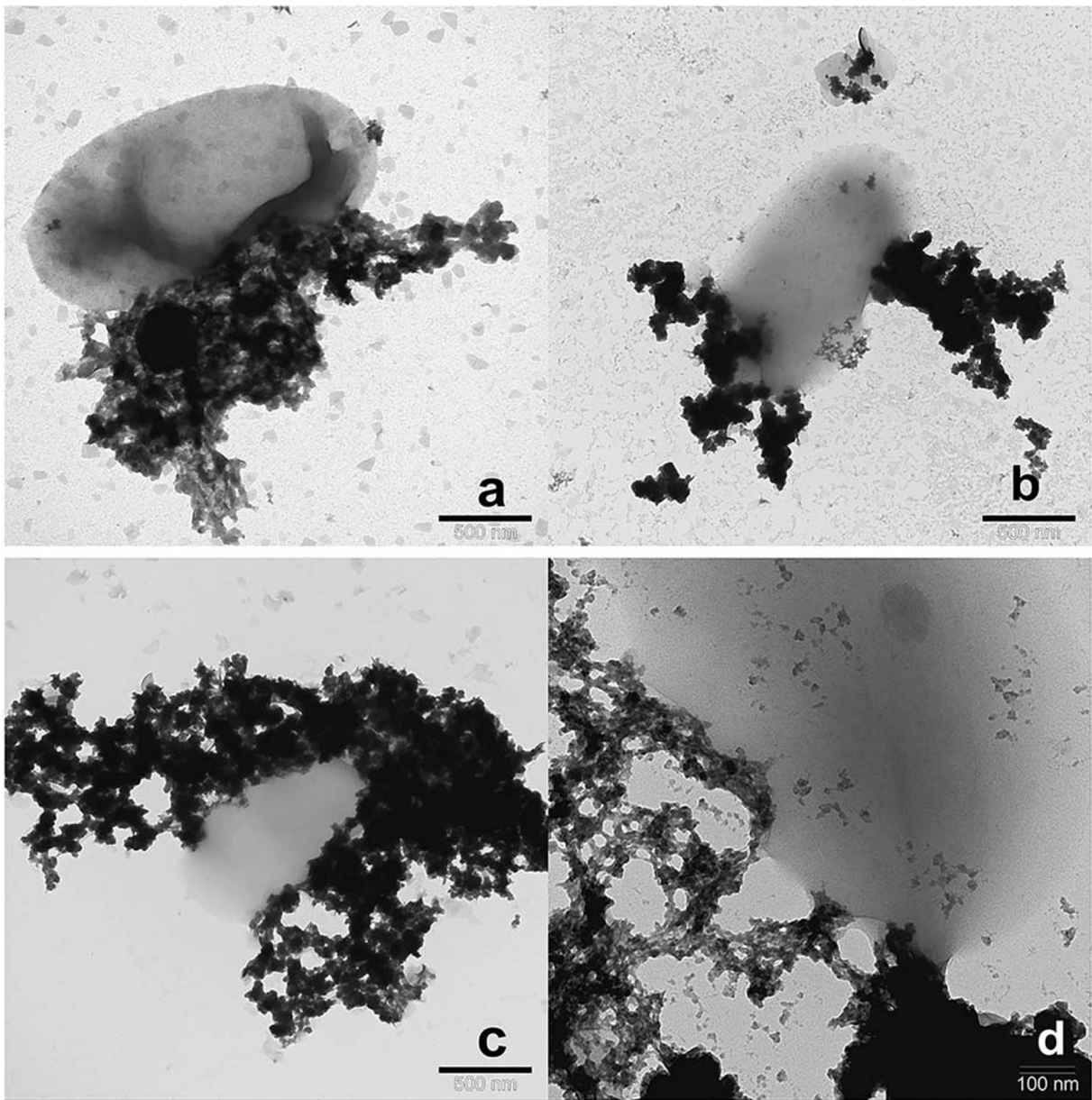


Fig. 5 TEM images from the gradient band of **a** *E. coli* K-12-captured $\text{Fe}_3\text{O}_4@Au$, **b–d** *E. coli* K-12-captured CdTe/MPA@ch with **a–c** $\times 50,000$ and **d** $\times 150,000$ magnification

Results of bacteria-nanoparticle band migrations

Depending on the differences in size and density of bacteria, particle, and bacteria-captured nanoparticle, inequality of buoyant density of the bands was predicted to be $d_{\text{particle}} > d_{\text{bacteria-particle}} > d_{\text{bacteria}}$. It was seen that unconjugated $\text{Fe}_3\text{O}_4@Au$ particles exceeded 80% w/v

sucrose zone and precipitated at the bottom of the tube; however, bacteria-captured NP band remained at the 60–80% w/v sucrose interface of the gradient when applied centrifugation duration exceeded 1 h. Besides, unconjugated bacteria band remained on the 40–60% w/v sucrose interface depending on its lower buoyant density. For this reason, it was confirmed that bacteria-

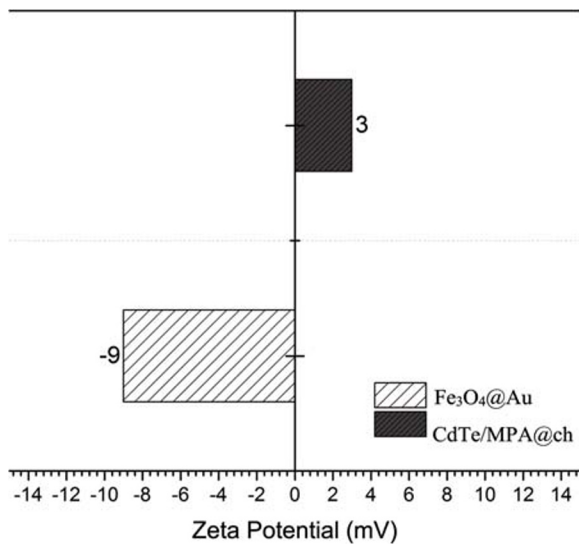


Fig. 6 Zeta potentials of Fe_3O_4 @Au NPs and CdTe/MPA@ch Qdots

NP bands have lower sedimentation rates than the unconjugated NPs.

In order to achieve quantification of bacteria-NP conjugate bands, optimum process (RCF, time) parameters were examined in the appropriate gradient that consists of 1 ml each of 40%, 50%, 60%, 70%, and 80% (w/v) sucrose. In accordance with our predictions, it was clearly seen from Fig. 8a that unconjugated NP band moved further than *E. coli* K-12-captured band as a result of its' higher sedimentation rate. After 10 min of centrifugation, the differentiation of migration distance

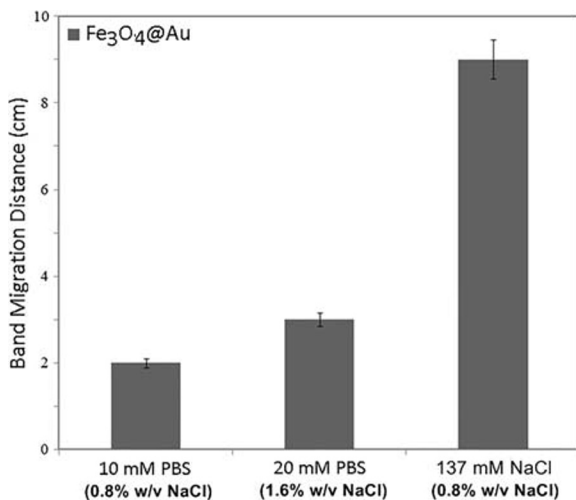


Fig. 7 Band migration graphs for the comparison of buffer solutions in the sucrose gradient that consists of 10%, 15%, 20%, 30%, 40%, and 80% (w/v) sucrose

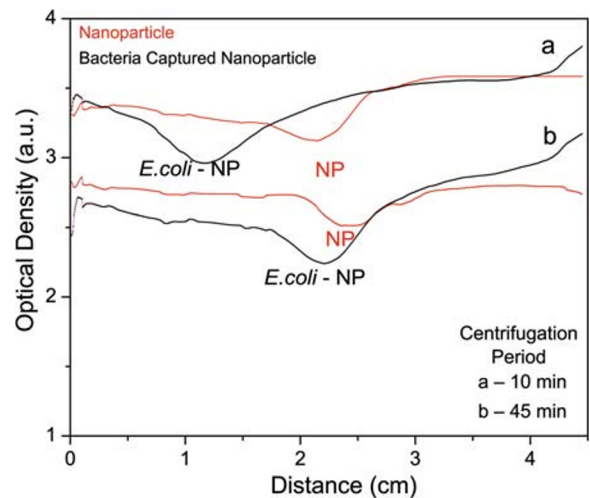


Fig. 8 Time-dependent optical measurement of Fe_3O_4 @Au NP and 10^8 cfu/ml of *E. coli*-captured NP bands, after **a** 10 min and **b** 45 min of centrifugation at $1000\times g$

of bacteria-conjugated NP band and unconjugated NP band was found to be available for the analysis. It is known that sedimentation velocity decreases significantly when viscosity of the solvent increases (Sheehan 2013). When centrifugation period increased to 45 min, peak maximum of the curves converged as a result of lower sedimentation velocities of bands towards the denser sucrose gradient zone (Fig. 8b). According to our results, appropriate centrifugation time should be 10 min for Fe_3O_4 @Au in the chosen gradient concentrations.

In addition, when bacteria concentration decreased from 108 to 105 cfu/ml of *E. coli* K-12, peak maximums of band migrations meet as shown in Fig. 9a. It was seen that quantification of bacterial concentration is not suitable by using these gradient parameters. When the centrifugation period increased to 45 min, unconjugated NPs precipitated on the sidewalls and the bottom of the tube (Fig. 9). Consequently, Gaussian distribution disappeared and secondary peaks from *E. coli*-captured NP curve were observed. Although main peak of 10^5 cfu/ml of *E. coli*-captured NP band remained in the same sucrose density zone, unconjugated NPs precipitated at the bottom of the tube and separated from the conjugated NP band (Fig. 9b).

Chitosan-capped quantum dots were found to be the most advantageous tool among the nanoparticles that we utilized to identify conjugated NP bands. The reasons are that Qdots have light emitting property that enables significant band tracking under dark light, and have an

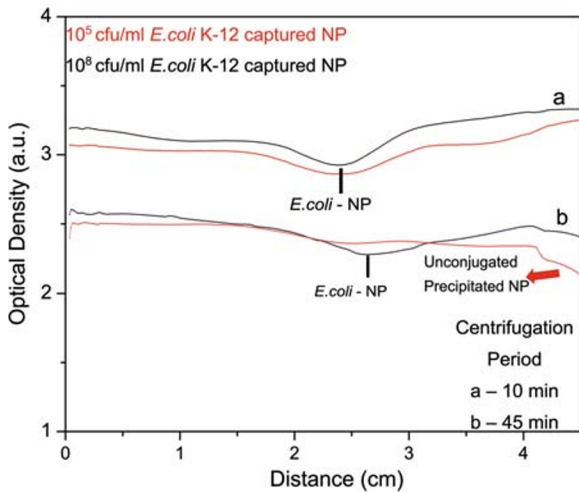


Fig. 9 Time- and bacterial concentration-dependent optical measurement of 10^5 – 10^8 cfu/ml of *E. coli* K-12-captured Fe_3O_4 @Au NP bands, after **a** 10 min and **b** 45 min of centrifugation period

attractive polymeric surface that allows strict adherence to bacteria. The sizes of chitosan-capped Qdots are smaller than other nanoparticles used; however, Qdots have shown apparent band shift due to the huge aggregation mechanism of attractive polymeric surface. To prevent the breaking of non-specific adherence between bacteria and Qdot, centrifugation was conducted at low RCF in minimum process time. When the duration of centrifugation increased, bacteria-captured CdTe/MPA@ch band did not separate into two or more bands. However, particles dispersed more in the gradient, and band structure disappeared. Therefore, optimum process parameters were determined by observing the change between the sequential tubes of bacteria-captured NPs. While utilizing Fe_3O_4 @Au NPs and

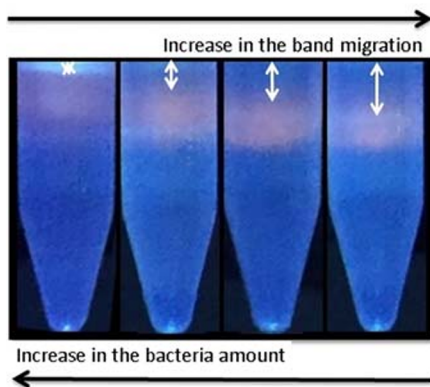


Fig. 10 An illustration of 10^5 – 10^8 cfu/ml of *E. coli* K-12-captured Qdot band migrations in the gradient of 40%, 50%, 60%, 70%, and 80% (w/v) sucrose, after 3 min of centrifugation at $500\times g$

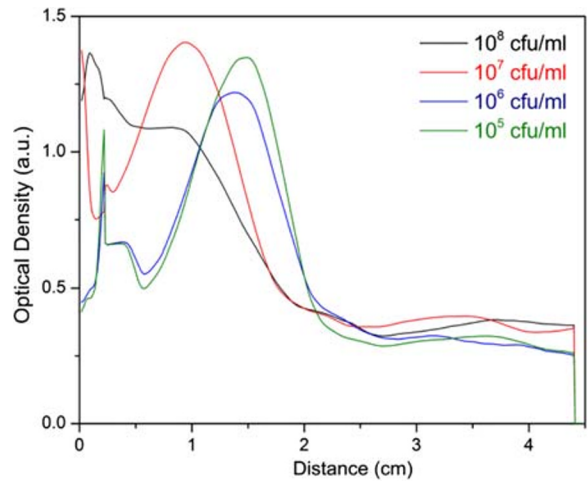


Fig. 11 Bacterial concentration-dependent band migrations of *E. coli* K-12-captured Qdots, after 3 min of centrifugation at $500\times g$

CdTe/MPA@ch NPs to evaluate bacteria conjugate movement, optimum process parameters of $1000\times g/10$ min and $500\times g/3$ min were determined, respectively.

An illustration of bacteria-captured Qdot bands under dark light was given in Fig. 10. Bacteria-captured Qdots showed greater floating tendency and lower sedimentation velocity with respect to the increase in bacterial concentration. It was seen that high concentration of bacteria-captured Qdot band moved slower than the low bacteria-conjugated Qdot band. This situation enabled the quantification of bacteria bands at an optimum given centrifugation time.

The bacterial concentration-dependent optical density-distance graph of *E. coli*-captured Qdot bands

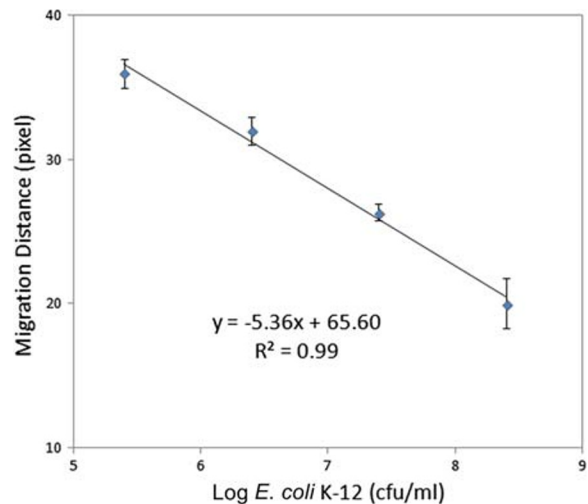


Fig. 12 Calibration curve of *E. coli* K-12-captured Qdots

was given in Fig. 11. It was seen that bacteria-captured Qdot band remained Gaussian curve ($R^2 > 0.83$) during rate-zonal centrifugation process. It was clearly seen that distance of band migration decreased when bacterial concentration increases. The quantification of bacteria-Qdot bands achieved only after 3 min of centrifugation at $500\times g$.

Calibration curve of bacteria-captured Qdot was obtained within the range of 10^5 – 10^8 cfu/ml of *E. coli* K-12 (Fig. 12). The limit of quantification value, which is a reliable measurement limit of a sensor, was calculated as 3.4×10^5 cfu/ml of *E. coli* K-12.

Conclusion

In this study, a new analytical method was developed with the use of nanoparticles, sucrose gradient centrifugation, and an easy optical setup. It is a novel idea to detect and enumerate bacteria by means of buoyancy tendency and sedimentation velocity sorting of “bacteria-captured NPs” in sucrose gradient. Whole parameters of gradient system were examined to obtain narrow moving bands. According to our findings, it was seen that optimum gradient centrifugation parameters should be adjusted to achieve sensitive enumeration of bacteria when using different nanoparticles. Physical comparison of synthesized NPs demonstrated that denser CdTe/MPA@ch and $Fe_3O_4@Au$ were preferred for rate-zonal centrifugation of NP-bacteria conjugates in the gradient of 40%, 50%, 60%, 70%, and 80% (w/v) sucrose dissolved in PBS. It was seen that chitosan-capped Qdots show apparent band shifts depending on the bacterial concentration. The reason is that they have attractive polymeric surface that allows strict adherence to bacteria. Besides, the light emitting property of Qdots enables significant band tracking under dark light.

In conclusion, an easy-handling and rapid bacteria quantification methodology was developed without using specific antibody-antigen interactions and time-consuming washing steps of immunoassay methods. This new buoyancy and optical density-based gradient method is a promising method for detecting bacteria in less than 50 min of total detection time. Moreover, by making modifications on NP surfaces with affinity reagents, this NP-based quantification method has potential for future specific bacteria detection.

Acknowledgments Authors would like to thank members of Real Time Monitoring Research Group (RTMRG), especially Dr. Haslet Eksi Kocak and Emine Kubra Tayyarcan for their help during this research at Hacettepe University. Authors would also like to thank Dr. Nusret Ertas for the synthesis of CdTe quantum dots at Gazi University.

Compliance with ethical standards

Conflict of interest The authors declare that they have no conflict of interest.

References

- Akbulut O, Mace CR, Martinez RV, Kumar AA, Nie Z, Patton MR, Whitesides GM (2012) Separation of nanoparticles in aqueous multiphase systems through centrifugation. *Nano Lett* 12:4060–4064. <https://doi.org/10.1021/nl301452x>
- Amir A, Babaeipour F, McIntosh DB, Nelsona DR, Suckjoon Junb S (2014) Bending forces plastically deform growing bacterial cell walls. *Proceedings of the National Academy of Science of the United States of America* 111:5778–5783. <https://doi.org/10.1073/pnas.1317497111>
- Baniukevic J, Boyaci IH, Bozkurt AG, Tamer U, Ramanavicius A, Ramanaviciene A (2013) Magnetic gold nanoparticles in SERS-based sandwich immunoassay for antigen detection by well oriented antibodies. *Biosens Bioelectron* 43:281–288. <https://doi.org/10.1016/j.bios.2012.12.014>
- Buckley DH, Huangyutham V, Hsu SF, Nelson TA (2007) Stable isotope probing with ^{15}N achieved by disentangling the effects of genome G+C content and isotope enrichment on DNA density. *Appl Environ Microbiol* 73:3189–3195
- Dogan U, Kasap E, Cetin D, Suludere Z, Boyaci IH, Turkyilmaz C, Ertas N, Tamer U (2016) Rapid detection of bacteria based on homogenous immunoassay using chitosan modified quantum dots. *Sensors Actuators B Chem* 233:369–378. <https://doi.org/10.1016/j.snb.2016.04.081>
- Écija-Arenas Á, Román-Pizarro V, Fernández-Romero JM, Gómez-Hens A (2016) Separation and purification of hydrophobic magnetite-gold hybrid nanoparticles by multiphase density gradient centrifugation. *Microchim Acta* 183:2005–2012. <https://doi.org/10.1007/s00604-016-1838-z>
- Ekici G, Dumen E (2019) *Escherichia coli* and food safety. In: *The Universe of Escherichia coli*. IntechOpen. <https://doi.org/10.5772/intechopen.82375>
- Fissan H, Simon Ristig S, Kaminski H, Asbach C, Epple M (2014) Comparison of different characterization methods for nanoparticle dispersions before and after aerosolization. *Anal Methods* 2014:7324–7334. <https://doi.org/10.1039/C4AY01203H>
- Gao J, Huang X, Liu H, Zan F, Ren J (2012) Colloidal stability of gold nanoparticles modified with thiol compounds: bioconjugation and application in cancer cell imaging. *Langmuir* 28:4464–4471. <https://doi.org/10.1021/la204289k>
- Guvenc B, Basaran-Akgul N, Temur E, Tamer U, Boyaci IH (2011) SERS-based sandwich immunoassay using antibody coated

- magnetic nanoparticles for Escherichia coli enumeration. *Analyst* 136:740–748. <https://doi.org/10.1039/C0AN00473A>
- Hu C, Chen Y (2015) Uniformization of silica particles by theory directed rate-zonal centrifugation to build high quality photonic crystals. *Chem Eng J* 271:128–134
- Jerri HA, Sheehan WP, Snyder CE, Velegol D (2010) Prolonging density gradient stability. *Langmuir: the ACS journal of surfaces and colloids* 26:4725–4731. <https://doi.org/10.1021/la903616p>
- Kumar A, Dixit CK (2017) Methods for characterization of nanoparticles. *Advances in Nanomedicine for the Delivery of Therapeutic Nucleic Acids* Woodhead Publishing:43–58. <https://doi.org/10.1016/B978-0-08-100557-6.00003-1>
- Kowalczyk B, Lagzi I, Grzybowski BA (2011) Nanoseparations: strategies for size and/or shape-selective purification of nanoparticles. *Curr Opin Colloid Interface Sci* 16:135–148. <https://doi.org/10.1016/j.cocis.2011.01.004>
- Li Z, Ma J, Ruan J, Zhuang X (2019) Using positively charged magnetic nanoparticles to capture bacteria at ultralow concentration. *Nanoscale Res Lett* 14(1):195. <https://doi.org/10.1186/s11671-019-3005-z>
- Lin L, Choundhary A, Bavishi A, Ogbonna N, Maddux S (2012) Use of sucrose gradient method for bacterial cell cycle synchronization. *J Microbiol Biol Educ*:50–53
- Liu J, Lu Y (2005) Fast colorimetric sensing of adenosine and cocaine based on a general sensor design involving aptamers and nanoparticles. *Angew Chem Int Ed Eng* 45:90–94. <https://doi.org/10.1002/anie.200502589>
- Liu J, Lu Y (2006) Preparation of aptamer-linked gold nanoparticle purple aggregates for colorimetric sensing of analytes. *Nat Protoc* 1:246–252. <https://doi.org/10.1038/nprot.2006.38>
- Mace CR, Akbulut O, Kumar AA, Shapiro ND, Derda R, Patton MR, Whitesides GM (2012) Aqueous multiphase systems of polymers and surfactants provide self-assembling step-gradients in density. *J Am Chem Soc* 134:9094–9097. <https://doi.org/10.1021/ja303183z>
- Menesatti P, Angelini C, Pallottino F, Antonucci F, Aguzzi J, Costa C (2012) RGB color calibration for quantitative image analysis: the “3D thin-plate spline” warping approach. *Sensors* 12(6):7063–7079. <https://doi.org/10.3390/s120607063>
- Mezger A, Fock J, Antunes P, Österberg F, Boisen A, Nilsson M, Hansen MF, Ahlford A, Donolato M (2015) Scalable DNA-based magnetic nanoparticle agglutination assay for bacterial detection in patient samples. *ACS Nano* 9:7374–7382. <https://doi.org/10.1021/acs.nano.5b02379>
- Omi N, Tokuda Y, Ikeda Y, Ueno M, Mori K, Sotozono C, Kinoshita S, Nakano M, Tashiro K (2017) Efficient and reliable establishment of lymphoblastoid cell lines by Epstein-Barr virus transformation from a limited amount of peripheral blood. *Sci Rep* 7:43833. <https://doi.org/10.1038/srep43833>
- Ou F, McGoverin C, Swift S, Vanholsbeeck F (2019) Near real-time enumeration of live and dead bacteria using a fibre-based spectroscopic device. *Sci Rep* 9:4807. <https://doi.org/10.1038/s41598-019-41221-1>
- Pathak P, Ramrakhiani M, Mor P (2015) Influence of temperature of precursor solution on structural and optical properties of nanocrystalline CdTe thin films deposited by chemical bath deposition technique *International Journal of Scientific & Engineering Research* 6
- Portoso M, Ragazzini R, Brenčić Ž, Moiani A, Michaud A, Vassilev I, Wassef M, Servant N, Sargueil B, Margueron R (2017) PRC2 is dispensable for HOTAIR-mediated transcriptional repression. *EMBO J*:1–14. doi:<https://doi.org/10.15252/emj.201695335>
- Prantner AM, Chen J, Murray CB, Scholler N. (2012) Coating evaluation and purification of Monodisperse, Water-soluble, magnetic nanoparticles using sucrose density gradient ultracentrifugation chemistry of materials 24:4008–4010. doi:<https://doi.org/10.1021/cm302582z>
- Qi X, Li M, Kuang Y, Wang C, Cai Z, Zhang J, You S, Yin M, Wan P, Sun X (2015) Controllable assembly and separation of colloidal nanoparticles through a one-tube synthesis based on density gradient centrifugation chemistry – a european journal 21:7211–7216. doi:<https://doi.org/10.1002/chem.201406507>
- Rodoplu D, Boyaci IH, Bozkurt AG, Eksi H, Zengin A, Tamer U, Aydogan N, Ozcan S, Tugcu-Demiroz F (2015) Quantitative characterization of magnetic mobility of nanoparticle in solution-based condition. *Curr Pharm Des* 21:5389–5400. <https://doi.org/10.2174/1381612821666150917092327>
- Schachman HK (1959) *Ultracentrifugation in biochemistry*. Academic Press Newyork
- Seo SH, Lee YR, Ho Jeon J, Hwang YR, Park PG, Ahn DR, Han KC, Rhie GE, Hong KJ (2015) Highly sensitive detection of a bio-threat pathogen by gold nanoparticle-based oligonucleotide-linked immunosorbent assay. *Biosens Bioelectron* 64:69–73. <https://doi.org/10.1016/j.bios.2014.08.038>
- Sharma V, Park K, Srinivasarao M (2009) Shape separation of gold nanorods using centrifugation. *Proc Natl Acad Sci U S A* 106:4981–4985. <https://doi.org/10.1073/pnas.0800599106>
- Sheehan D (2013) *Physical biochemistry: principles and applications*. John Wiley & Sons
- Sik O, Grmela L (2013) Photoconductivity of CdTe semiconductor radiation detectors *International Journal Of Computer Science And Electronics Engineering* 1
- Sun X, Tabakman SM, Seo WS, Zhang L, Zhang G, Sherlock S, Bai L, Dai H (2009) Separation of nanoparticles in a density gradient: FeCo@C and gold nanocrystals *Angewandte Chemie International Edition* 48:939–942 <https://doi.org/10.1002/anie.200805047>
- Suresh AK, Pelletier DA, Moon JW, Phelps TJ, Doktycz MJ (2015) Size-separation of silver nanoparticles using sucrose gradient centrifugation. *J Chromatogr Sep Tech*:6. <https://doi.org/10.4172/2157-7064.1000283>
- Tamer U, Gundogdu Y, Boyaci IH, Pekmez K (2010) Synthesis of magnetic core-shell Fe₃O₄-Au nanoparticle for biomolecule immobilization and detection. *J Nanopart Res* 12:1187–1196. <https://doi.org/10.1007/s11051-009-9749-0>
- Tay CY, Setyawati MI, Leong DT (2017) Nanoparticle density: a critical biophysical regulator of endothelial permeability *acs nano* 11:2764–2772. doi:<https://doi.org/10.1021/acs.nano.6b07806>
- US Research Nanomaterials (n.d.-a) Gold (Au) Nanopowder / Nanoparticles (Au, 99.99+%, 50–100 nm)
- US Research Nanomaterials (n.d.-b) Iron Oxide (Fe₃O₄) Nanopowder / Nanoparticles (Fe₃O₄, 98+%, 20–30 nm)
- Wegner KD, Hildebrandt N (2015) Quantum dots: bright and versatile in vitro and in vivo fluorescence imaging biosensors. *Chem Soc Rev* 44:4792–4834. <https://doi.org/10.1039/c4cs00532e>

Wolfram Research I Density of the elements

Xiong B, Cheng J, Qiao Y, Zhou R, He Y, Yeung ES (2011) Separation of nanorods by density gradient centrifugation. *J Chromatogr A* 1218:3823–3829. <https://doi.org/10.1016/j.chroma.2011.04.038>

Yang C, Xie H, Li QC, Sun EJ, Su BL (2015) Adherence and interaction of cationic quantum dots on bacterial surfaces. *J*

Colloid Interface Sci 450:388–395. <https://doi.org/10.1016/j.jcis.2015.03.041>

Publisher's note Springer Nature remains neutral with regard to jurisdictional claims in published maps and institutional affiliations.